

Fig. 1. Power spectrum of output signals of the electromagnetic flowmeter.

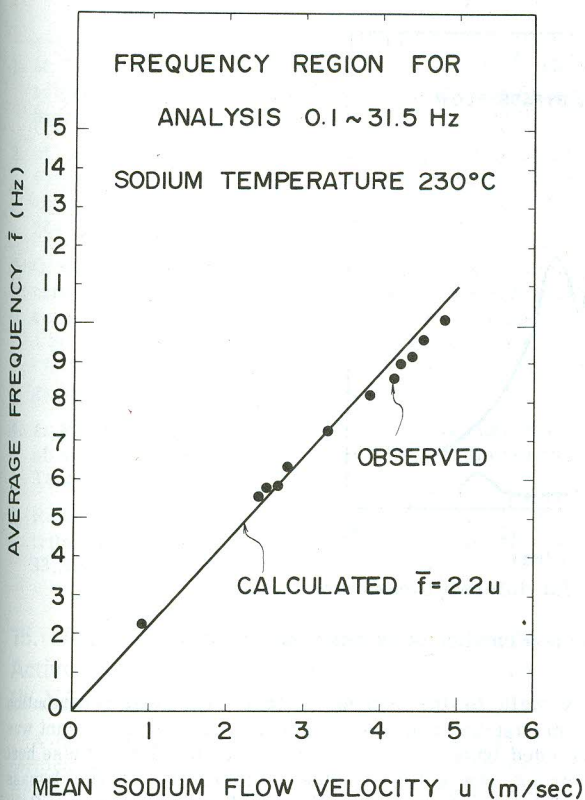


Fig. 2. Proportional relationship between average frequency of fluctuations included in output signals of the EMF and mean sodium flow velocity.

the calculated average frequencies agree well with the experimental ones.

1. A. C. RAPTIS and G. A. FÖRSTER, ANL-CT-76-8 (1975).
2. T. NIHEI and Y. MIMOTO, IAEA Specialists' Meeting on LMFBR, Warrington, United Kingdom (1976).

#### 14. Method for Detecting Bypass Coolant Boiling in Boiling Water Reactors, D. N. Fry (ORNL), W. T. King (Univ of Tenn), E. L. Machado (IEA-Brazil), F. J. Sweeney (Univ of Tenn)

Fluctuating signals from in-core neutron detectors in four boiling water reactors (BWRs) were analyzed to better understand the differences in the amplitude of neutron noise coherence spectra previously reported.<sup>1</sup> This investigation has led to a possible method for detecting boiling of bypass water in BWRs. A significant decrease in the coherence between signals from C and D local power range monitor (LPRM) detectors was observed when the core bypass coolant flow was reduced by plugging the holes in the core support plate—a modification made to reduce in-core instrument tube vibrations.

We hypothesized that reduced bypass flow caused boiling in the bypass region and that the onset of bypass boiling was at an elevation between the two detectors mentioned. Additional fluctuations in the downstream detector signals caused by bypass voids are not correlated to the upstream detector signals, thereby decreasing the coherence between the two signals.

All four plants included in the analysis had plugged bypass coolant holes. Three plants had only leakage flow in the bypass region, which is 6 to 8% of the total core flow. The fourth plant had coolant holes drilled in the lower tie plates of the fuel bundle, which increased the bypass flow to 10 to 12%. We analyzed simultaneous tape recordings of signals from the four in-core neutron detectors at each of the 31 to 43 LPRM locations in each plant. The detectors designated A, B, C, and D are located 18, 54, 90, and 126 in., respectively, from the fuel bundle inlet.

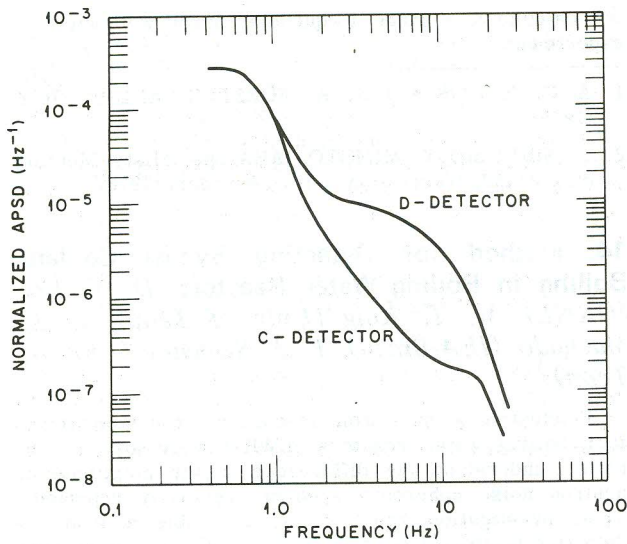
Figure 1 compares typical, normalized auto-power spectral densities (APSDs) of the C and D detector signals and their coherence in plants with 6 to 8% bypass flow with APSDs and coherence typical of the plant with 10 to 12% bypass flow. With 6 to 8% bypass flow, the amplitude of the noise spectrum of the D detector from 1 to 10 Hz is almost an order of magnitude larger than that of the C detector (Fig. 1a), whereas with 10 to 12% bypass flow, the C and D detector noise spectra are similar in the same frequency range (Fig. 1b).

Normally, the major contributors to neutron noise in the frequency range from 1 to 10 Hz are steam voids in the fuel channel boxes. Most of these voids are formed below the C and D detectors, such that both detectors detect some of the same voids. Therefore, the C and D detector signals are highly coherent, as in the case of the plant with 10 to 12% bypass flow (Fig. 1c). In fact, other investigators<sup>2,3</sup> have used these correlated neutron noise signals to infer the steam-void velocity and void fraction in the channel boxes in operating BWRs.

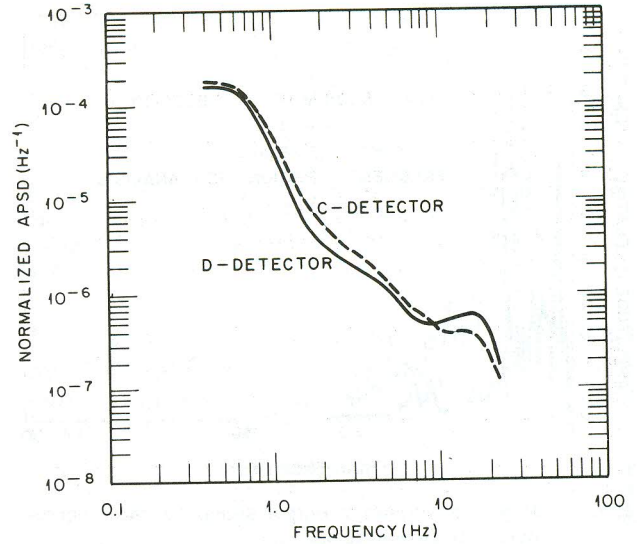
On the other hand, the added noise at the D detector location (presumably due to void formation in the bypass flow between the C and D detectors) in plants with 6 to 8% bypass flow is not correlated with the C detector signal,

found in Fig. 2 within an accuracy of  $\pm 6\%$  in the sodium flow velocity region of 0.87 to 4.7 m/s. From the analyzed results, it is seen that the average frequency method is useful for calibration of an electromagnetic flowmeter.

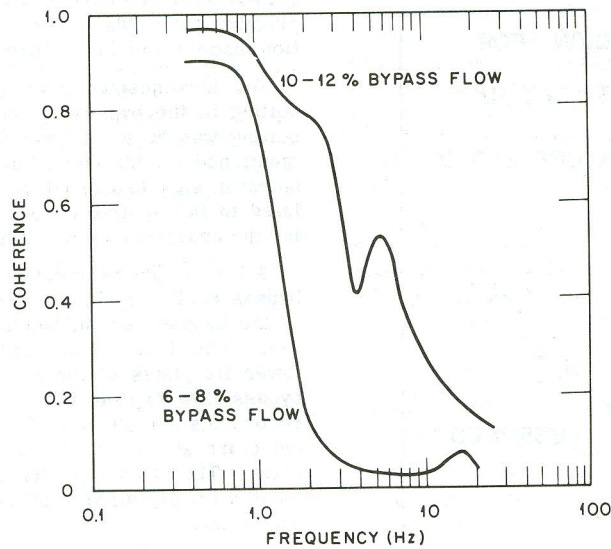
The authors tried to calculate the average frequency of the fluctuations of the sodium flow velocity on the basis of the mixing length hypothesis by Prandtl. The calculated average frequencies of the fluctuations are compared with the experimental ones in Fig. 2. It is found in Fig. 2 that



(a) Power spectrum for bypass flow of 6 to 8%.



(b) Power spectrum for bypass flow of 10 to 12%.



(c) C-D detector coherence spectra for different bypass flows.

Fig. 1. BWR-4 in-core neutron noise as a function of bypass flow.

thus resulting in the low coherence between the C and D detector signals (Fig. 1c).

A complicating factor in our analysis was that the plant with the greater bypass flow also had a different fuel design ( $8 \times 8$  fuel pin array, instead of  $7 \times 7$ ). However, because the A, B, and C detector signatures are similar in plants with either type of fuel, we do not believe this different fuel design caused the difference in the noise at the D detector location.

To test our hypothesis of bypass boiling, we performed a thermal-hydraulic calculation to estimate the elevation at which bypass boiling occurs as a function of the bypass flow rate. The fuel bundle coolant temperature was calculated using a code developed by Mills,<sup>4</sup> with a typical normalized traversing in-core probe (TIP) trace providing the power shape. The fuel bundle temperature and flow rates, together with the bypass flow rates and inlet conditions, were used to calculate the amount of heat conducted from the fuel bundle coolant, through the fuel

box wall, to the bypass coolant. The heat contribution from fast-neutron moderation in the bypass coolant was included based on the work by Carlson.<sup>5</sup> From these heat sources, we estimated the temperature of the bypass coolant as a function of elevation and bypass flow. Figure 2 shows that for 6 to 8% bypass flow the average bypass coolant temperature reached saturation temperature (bulk boiling) at  $\sim 100$  to 126 in. (between the C and D detectors). For bypass flows greater than  $\sim 9\%$ , the saturation temperature was not reached below the core outlet.

We conclude that reduced bypass flow caused boiling in the bypass region, and this boiling caused the observed differences in neutron noise signatures. These results suggest that, with the aid of the TIPs, the axial location at which bypass boiling occurs can be determined. With additional measurements and more refined thermal-hydraulic calculations, it might be possible to infer the bypass void fraction, which is of interest in the safety evaluation of BWRs.

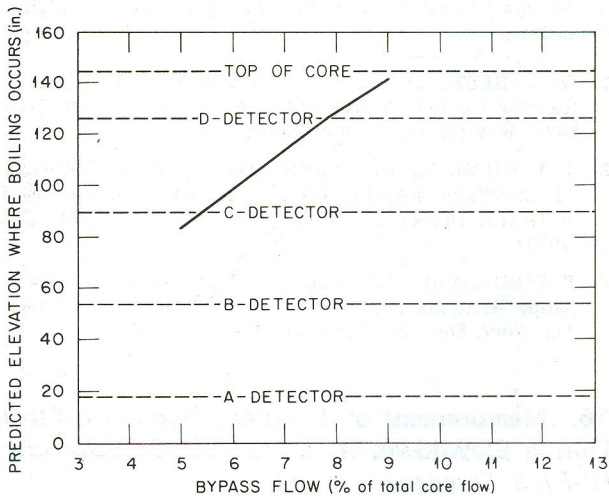


Fig. 2. Core elevation where bypass coolant bulk boiling is predicted to occur.

1. M. V. MATHIS, C. M. SMITH, and D. N. FRY, "Characterization Studies of BWR-4 Neutron Noise Analysis Spectra," *Trans. Am. Nucl. Soc.*, **27**, 677 (1977).
2. M. ASHRAFF ATTA et al., "Determination of Void Fraction Profile in a Boiling Water Reactor Channel Using Neutron Noise Analysis," *Nucl. Sci. Eng.*, **66**, 2, 264 (1978).
2. G. KOSÁLY et al., "Investigation of the Local Component of the Neutron Noise in a BWR and Its Application to the Study of Two-Phase Flow," *Proc. OECD (NEA) CSBI/NEACRP Specialists' Mtg. Reactor Noise (SMORN II)*, CSNI Report No. 22/NEACRP-U-81, Pergamon Press, Ltd., Oxford, England (1977).
4. L. MILLS, "An Investigation of the Thermal Aspects of a Boiling Water Reactor," MS Thesis, University of Tennessee, Knoxville (Mar. 1968).
5. R. G. CARLSON and D. R. GOTT, "Bypass Flow Distribution in a Boiling Water Reactor," *Nucl. Technol.*, **33**, 161 (1977).

### 15. An Automatic On-Line Reactor Coolant Activity Monitoring System, M. E. Crozter (W-NES), W. J. Bestoso (Bailey Controls)\*

A minicomputer-based system has been developed to perform continuous, automatic on-line activity measurements of reactor coolant.<sup>1,2</sup> The system was designed to reduce the routine manual sampling effort at nuclear power plants, especially during load follow and shutdown operations. Compliance with plant technical specifications is continuously monitored by automatically updating such parameters as the average beta-gamma energy per disintegration and dose equivalent <sup>131</sup>I. This reactor coolant activity monitoring system (RCAMS) provides greater sampling and analytical capability than a recently described system which used a batch sampling process and monitored only radioiodines.<sup>3</sup> The RCAMS development effort was supported by the Empire State Electric Energy Research Corporation.

A diagram of the RCAMS is shown in Fig. 1. The delay line reduces the <sup>15</sup>N gamma activity and delayed-

neutron activity to negligible levels. The internal surface of the sample section is either electropolished or lined with quartz tubing to minimize crud deposition. After pulses from the GeLi detector are processed, a mini-computer calculates net peak areas at preselected energies from the resulting gamma-ray spectrum and converts them to specific isotopic activities. Other operational modes print the raw spectral data and list peak areas by energy.

Forty or more preselected radionuclides can be processed and provisions exist for correcting each nuclide for a single interference. Special indications or "flags" are printed out for each radionuclide if its activity exceeds a preset value, or changes by a predetermined fraction over the last flagged value, or if the photopeak was not found at the preset energy. Report formats and operating sequences are flexible. For example, the system can automatically print out a daily activity summary for all preselected radionuclides and a weekly list of all gamma peaks found in the spectrum while simultaneously performing a trend analysis, reporting only "flagged" radionuclides.

The RCAMS was tested at a plant during a refueling shutdown and the results were compared with manual chemistry analysis. Figure 2 is an example of the generally excellent agreement obtained. The difference between manual sampling and RCAMS for <sup>58</sup>Co may be due to plateout in the samples shipped to the Westinghouse laboratory, since manual samples analyzed at the plant agreed with the RCAMS <sup>58</sup>Co activity. The Compton background measured at power before plant shutdown was used to calculate the minimum detectable activities for selected radionuclides. Table I lists the activities corresponding to 2 $\sigma$  levels above background for a 1-h counting time. This minimum level was compared to

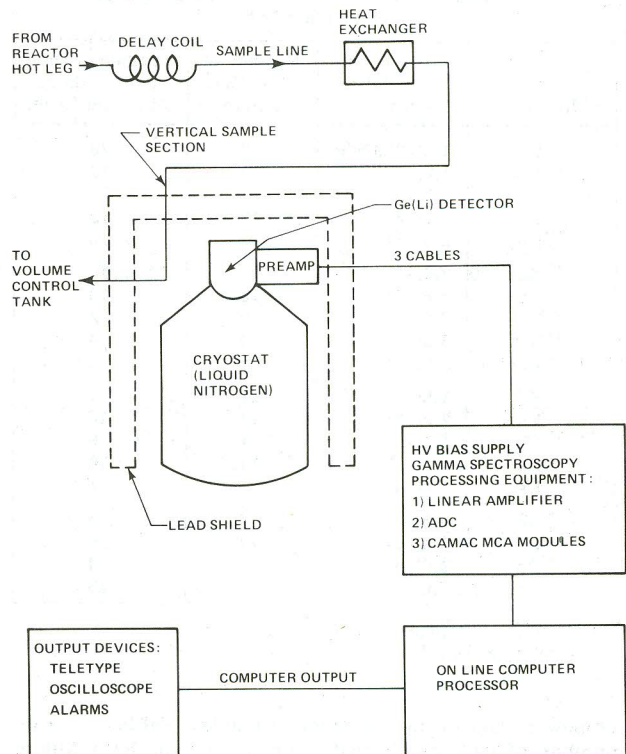


Fig. 1. Diagram of reactor coolant activity monitoring system (RCAMS).

\*Work performed while at Westinghouse PWRSD.